

THE PERFORMANCES OF MIXED EWMA-CUSUM CONTROL CHARTS BASED ON MEDIAN-BASED ESTIMATORS UNDER NON-NORMALITY

Nor Fashihah Mohd Noor^{a,b*}, Ayu Abdul-Rahman^a, Abdu Mohammed Ali Atta^c

^aDepartment of Mathematics & Statistics, School of Quantitative Sciences, Universiti Utara Malaysia, 06010 UUM Sintok, Kedah, Malaysia

^bInstitute of Engineering Mathematics, Universiti Malaysia Perlis (UniMAP), 02600 Arau, Perlis, Malaysia

^cDepartment of Economic and Political Science, Hodeidah University, P.O. Box 3114 Yemen

Article history

Received

24 May 2023

Received in revised form

1 September 2023

Accepted

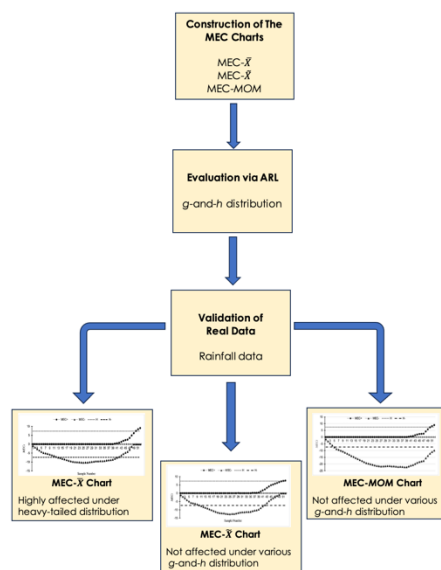
5 September 2023

Published Online

20 December 2023

*Corresponding author
norfashihah@unimap.edu.my

Graphical Abstract



Abstract

Exponentially weighted moving average (EWMA) and cumulative sum (CUSUM) charts have been regularly used to monitor small process mean shifts. More recently, a mixture of EWMA and CUSUM charts known as mixed EWMA-CUSUM (MEC) control chart has been introduced for better small shift detection. However, like its predecessor, the MEC chart requires the normality assumption to ensure optimal performances. In the presence of outliers, which is the cause of non-normality, the parameters of the chart may be overestimated, leading to an unreliable monitoring process. To mitigate this problem, this paper employed median-based estimators namely, the median and modified one-step M-estimator (MOM), to control the location parameter via the MEC control chart. In this study, the performance of robust MEC charts for Phase II monitoring of location was compared with the standard MEC chart that is based on the sample mean. The performance of the robust MEC charts in terms of the average run length (ARL) on various g -and- h distributions clearly shows that a robust MEC chart based on the MOM estimator performs well regardless of the distributional shapes.

Keywords: Non-normal, EWMA chart, CUSUM chart, Mixed EWMA-CUSUM chart, robust

Abstrak

Carta purata bergerak berpemberat eksponen (EWMA) dan carta hasil tambah longgokan (CUSUM) sering digunakan untuk memantau anjakan kecil min proses. Terkini, campuran carta EWMA dan CUSUM yang dikenali sebagai carta kawalan campuran EWMA-CUSUM (MEC) telah diperkenalkan bagi meningkatkan lagi prestasi carta. Namun, seperti pendahulunya, carta MEC memerlukan andaian normal untuk memastikan prestasi yang optimum. Apabila terdapat titik terpencil, yang merupakan punca ketidaknormalan, parameter carta mungkin dianggarkan lebih tinggi yang boleh menyebabkan ketidakbolehpercayaan pada proses pemantauan. Bagi mengurangkan masalah ini, kertas kerja ini menggunakan penganggar berasaskan median iaitu median dan penganggar-M satu langkah terubah suai (MOM) untuk mengawal parameter lokasi melalui carta kawalan MEC. Dalam kajian ini, prestasi carta-carta kawalan MEC teguh pada pemantauan Fasa II bagi lokasi dibandingkan dengan carta MEC piawai

berdasarkan min sampel. Prestasi carta-carta teguh dari segi purata panjang larian (ARL) pada pelbagai taburan g -dan- h jelas menunjukkan bahawa carta MEC teguh berdasarkan penganggar MOM memberikan prestasi yang baik tanpa mengira bentuk taburan.

Kata kunci: Tak normal, carta EWMA, carta CUSUM, carta campuran EWMA-CUSUM, teguh

© 2024 Penerbit UTM Press. All rights reserved

1.0 INTRODUCTION

Generally, a control chart is used to observe and conclude whether a process is in statistical control or otherwise. Ideally, the control chart shall signal as soon as possible when the process shifts into an out-of-control state. Shewhart [1] developed a control chart called the Shewhart control chart, which can be effectively used to monitor processes with large shifts. This chart is based on the present information of the process and thus, it is categorized as a memoryless control chart. Due to this feature, the Shewhart chart is less sensitive in monitoring small process shifts [2, 3, 4, 5, 6].

To improve Shewhart's performance in monitoring small to moderate shifts, the synthetic chart was introduced [7]. Yet, it fails to outperform the CUSUM and EWMA charts when the change in the process is relatively small [8]. This is because the synthetic chart also neglects past information, just like the Shewhart chart.

In contrast, the CUSUM and EWMA charts, which are categorized as memory-type control charts, utilize past and current information of the data in the process. This feature makes the CUSUM and EWMA charts superior to the memoryless charts, i.e., the Shewhart and synthetic charts, in detecting small and moderate shifts [9, 10, 11, 12]. Recently, to improve the performance of the memory-type control charts, Abbas *et al.* [13] proposed to combine the EWMA and CUSUM structures into one new chart. This new chart is known as the MEC control chart.

It is well known that the standard estimators, i.e., the sample mean and standard deviation, are sensitive to outliers and yet, they define the construction of the abovementioned memoryless and memory-type control charts. As such, the performance of the charts may deteriorate due to the existence of outliers. Several researchers have claimed that control charts constructed using robust estimators have performed well under non-normality [14, 15, 16, 17]. Castagliola [18], for example, introduced the median chart via the EWMA control structure. Meanwhile, the study by Abdul Rahman *et al.* [19] explored the effects of utilizing robust location estimators, specifically the median and Hodges-

Lehmann, on the performance of the CUSUM chart. In another robust study by Abdul-Rahman *et al.* [20], the researchers employed robust location and scale estimators namely, an automatic trimmed mean and median absolute deviation about the median (MADn), in Phase I of the EMWA chart. These robust control charts showed an improvement in the CUSUM and EWMA charts' performances, particularly in detecting out-of-control status when the data set is contaminated.

More recently, Abdul-Rahman [21] proposed to control the location parameter via the median based estimators, i.e., MOM and its winsorized version, via the synthetic charting structure under non-normality, specifically using the g -and- h distributions. The finding indicates good in-control robustness when the median based synthetic charts were designed for moderate and large shifts. Yet, due to the characteristic of the memoryless chart which only focuses on the present process information, the study claimed a lack of in-control robustness when the synthetic chart was designed for a small shift.

To mitigate this problem, this study employed median based estimators, i.e., the median and MOM, which possess the highest breakdown point, to replace the mean in constructing one of the memory-type charts, i.e., the MEC chart. The following sections explain in detail the structure of the MEC chart, together with the CUSUM and EWMA charts.

2.0 METHODOLOGY

2.1 Description of Cumulative Sum Control Chart

Introduced by Page [22], the CUSUM chart displays the cumulative data points of the present and previous samples in the process. Measurements of the samples are taken at a specified time and used to compute the CUSUM statistics, C_i^+ and C_i^- which are defined as follows:

$$C_i^+ = \max[0, (\hat{\theta}_i - \theta_0) - K_{\hat{\theta}} + C_{i-1}^+],$$

for $i = 1, 2, \dots, m;$ (1)

and

$$C_i^- = \min[0, (\hat{\theta}_i - \theta_0) + K_{\hat{\theta}} + C_{i-1}^-],$$

for $i = 1, 2, \dots, m$, (2)

where $\hat{\theta}$ is the location estimator and K is the reference value which can be adjusted to reflect the desired sensitivity in detecting shift in the process.

The initial values of the statistics, C_0^+ and C_0^- , are usually set equal to the target value, θ_0 . The standardized CUSUM control chart parameters are $K_{\hat{\theta}} = k \times \sigma_{\hat{\theta}}$ and $H_{\hat{\theta}} = h \times \sigma_{\hat{\theta}}$ where k and h are constants that correspond to a specific in-control average run length (ARL). Henceforth, the in-control ARL is denoted as ARL_0 . Typically, k is set to $\frac{\sigma_{\hat{\theta}}}{2}$. This approach makes the CUSUM more sensitive to the process shifts when the shift is relatively small [23].

2.2 Description of Exponentially Weighted Moving Average Control Chart

The idea of an EWMA control chart was originated by Roberts [24]. Each charting statistic in the EWMA chart signifies the weighted average of the present and all past subgroup values, giving more weight to current process data and less weight as the data get older. The EWMA charting statistic is defined as:

$$Z_i = \lambda \hat{\theta}_i + (1 - \lambda)Z_{i-1}, \quad \text{for } i = 1, 2, \dots, m, \quad (3)$$

where λ is a smoothing constant that can take any value between 0 and 1. The starting value, Z_{-1} , is typically set equal to the target mean value, θ_0 . The EWMA statistic, Z_i , is plotted against the upper control limit (UCL) and lower control limit (LCL) which are defined as follows:

$$UCL_i = \theta_0 + L_{\hat{\theta}} \sqrt{\text{Var}(\hat{\theta}) \frac{\lambda}{2-\lambda} (1 - (1-\lambda)^{2i})}, \quad (4)$$

and

$$LCL_i = \theta_0 - L_{\hat{\theta}} \sqrt{\text{Var}(\hat{\theta}) \frac{\lambda}{2-\lambda} (1 - (1-\lambda)^{2i})}, \quad (5)$$

where $L_{\hat{\theta}}$ is a positive coefficient value. This coefficient is usually set at a value that yields the pre-determined ARL_0 .

Abbas et al. [13] made one of the most recent contributions where the researchers combined the EWMA and CUSUM charts in creating the mixed EWMA-CUSUM (MEC) chart.

2.3 Description of Mixed EWMA-CUSUM Control Chart

The salient features of CUSUM and EWMA are combined in the MEC chart to enhance small shift detection [13]. The MEC two plotting statistics are given as:

$$MEC_i^+ = \max[0, (Z_i - \theta_0) - K_{\hat{\theta}} + MEC_{i-1}^+],$$

for $i = 1, 2, \dots, m$; (6)

and

$$MEC_i^- = \min[0, (Z_i - \theta_0) + K_{\hat{\theta}} + MEC_{i-1}^-],$$

for $i = 1, 2, \dots, m$, (7)

where Z_i denotes the EWMA statistic in Equation (3), i represents the sample number until m subgroups, and MEC_0^+ and MEC_0^- are the upper and lower MEC charting statistics, respectively. Both statistics are initially set to 0. Meanwhile, $K_{\hat{\theta}}$ is the time-varying reference value in the MEC chart. In Equation (8), the value of $\lambda \in (0, 1]$ and the initial value of Z_i is usually equal to the target mean value ($Z_0 = \theta_0$). The variance of Z_i , which was used in the computation of the parameters of the chart, is given as follows:

$$\text{Var}(Z_i) = \sigma_{\hat{\theta}}^2 \left[\frac{\lambda}{2-\lambda} (1 - (1-\lambda)^{2i}) \right]. \quad (8)$$

There are two standardized parameters, $K_{\hat{\theta},i} = k \times \sqrt{\text{Var}(Z_i)}$ and $H_{\hat{\theta},i} = h \times \sqrt{\text{Var}(Z_i)}$, where the notation $H_{\hat{\theta}}$ represents the control limit, k and h are the constants comparable to the one utilized in the standard CUSUM chart, which is the reference value and decision limit, respectively. The values of k and h are set to achieve the pre-determined ARL_0 . When i in the Equation (8) approaching infinity ($i \rightarrow \infty$), $\text{Var}(Z_i) = \sigma_{\hat{\theta}}^2 \left[\frac{\lambda}{2-\lambda} \right]$, the two quantities become $K_{\hat{\theta}} = k \times \sigma_{\hat{\theta}} \sqrt{\frac{\lambda}{2-\lambda}}$, and $H_{\hat{\theta}} = h \times \sigma_{\hat{\theta}} \sqrt{\frac{\lambda}{2-\lambda}}$.

In utilizing the MEC chart for detecting an out-of-control process, both of the charting statistics, i.e., MEC_i^+ and MEC_i^- are plotted against the control limit, $H_{\hat{\theta}}$. The process is said to be in statistical control if the two plotting statistics are randomly scattered between 0 and $H_{\hat{\theta}}$. If either of the charting statistics exceeds $H_{\hat{\theta}}$, the process is said to be out-of-control. Here, choices of h , the amount of shift, δ , and λ paired with a fixed value of k would give practitioners the pre-determined ARL_0 [13].

2.3.1 Robust Location Estimators

In this study, $\hat{\theta}_i$ in Equation (3) which later be used in computing the MEC charting statistics as demonstrated in Equation (6) and (7) were computed using two robust estimators namely, the median and MOM. The sample median is computed as follows:

$$\hat{\theta}_i = \begin{cases} X_{\frac{n+1}{2}}, & \text{if } n \text{ is odd} \\ \frac{1}{2} \left(X_{\frac{n}{2}} + X_{\frac{n+2}{2}} \right), & \text{if } n \text{ is even,} \end{cases} \quad (9)$$

where n is the sample size. Meanwhile, the MOM is computed as follows:

$$\hat{\theta}_i = \frac{\sum_{i=i_1+1}^{n-i_2} X_{(i)}}{n-i_1-i_2}, \quad (10)$$

where

$X_{(i)}$ = i th ordered observation;

i_1 = number of observations X_i such that $(X_i - M) < -K(MAD_n)$;

i_2 = number of observations X_i such that $(X_i - M) > K(MAD_n)$;

with M = median, $MAD_n = 1.4826 \text{ med}_i |x_i - \text{med}_j x_j|$ and $K = 2.24$.

3.0 RESULTS AND DISCUSSION

3.1 Case I: MEC Control Charts with Known Parameters

A Monte Carlo simulation analysis was carried out to assess the performance of the robust MEC charts based on the ARL. The ARL_0 assessed the in-control robustness of the MEC charts. Meanwhile, the true out-of-control condition was assessed via the out-of-control ARL (henceforth denoted as ARL_1). A good control chart would have a reasonably large ARL_0 when the process is in-control. Meanwhile, the ARL_1 is expected to be as small as possible when the process is out-of-control [5].

In this study, 10,000 datasets were generated using SAS 9.4 to compute the ARL where several variables were manipulated to mimic the most frequently encountered conditions in real life.

The g -and- h distribution was employed to manipulate the shapes of the distributions. Each distribution was subsequently paired with two different sample sizes, ($n = 5, 9$) and various amounts of shift, ($\delta = 0, 0.25, 0.5, 0.75, 1, 1.5, 2, 3$) to test the strengths and weaknesses of the proposed robust MEC charts against the standard MEC chart.

To generate data using the g -and- h distributions, it is necessary to follow the subsequent steps:

- i. Generate random variables following standard normal distribution, $Z_{ij} \sim N(0,1)$.
- ii. Transform the standard normal variables into random variables using an equation as follows:

$$X_{ij} = \begin{cases} \frac{\exp(gZ_{ij})-1}{g} \exp\left(\frac{hZ_{ij}^2}{2}\right), & g \neq 0 \\ Z_{ij} \exp\left(\frac{hZ_{ij}^2}{2}\right), & g = 0. \end{cases} \quad (11)$$

The parameters g and h are responsible for controlling the skewness and kurtosis, respectively. When $g = 0$ and $h = 0$, $X_{ij} = Z$ represents a standard normal distribution. As h gets larger, the tails of the distribution become heavier. The same goes for g , which controls the skewness. In this study, four different g -and- h distributions were generated as displayed in Table 1.

Table 1 The g -and- h distribution employed in the study

(g,h)	Description
(0,0)	Normal
(0,0.5)	Symmetric heavy tail
(0.5,0)	Skewed normal tail
(0.5,0.5)	Skewed heavy tail

In this study, the charting constants for the MEC charts, were derived for $k = 0.5$ and $\lambda = 0.13$ with the pre-determined ARL_0 set at 370 under $g = 0, h = 0$ distribution, which is the standard normal distribution. The charting constants for different n are listed in Table 2.

Table 2 The charting constants for different sample sizes (n) when process parameters are known

n	MEC-\bar{X}	MEC-\tilde{X}	MEC-MOM
5	28.02	28.30	28.15
9	27.85	28.13	28.08

3.1.1 Simulation Outcomes

In this study, two median based MEC charts were constructed via the usage of the median and MOM estimators. Respectively, these robust charts are denoted as the MEC- \tilde{X} and MEC-MOM charts whereby their performances were compared to the standard chart, henceforth denoted as the MEC- \bar{X} chart, based on the ARL. The results are displayed in Table 3.

Focusing on the normal distribution, when $g = 0$ and $h = 0$, all charts yield $ARL_0 = 370$ as they were initially designed in this study. In terms of the shift detection, all charts perform equally as shown by the ARL_1 in Table 3. Moreover, as n increases, the value of ARL_1 decreases for all charts, suggesting improvement in detecting shifts.

When $g = 0$ and $h = 0.5$, where the distribution is symmetric heavy-tailed, the in-control robustness of the MEC- \tilde{X} and MEC-MOM charts remain unaffected since the values of the ARL_0 are not much different than the pre-determined value of 370. On the other hand, the standard MEC- \bar{X} chart produces ARL_0 values that are significantly greater than 370, regardless of the sample sizes examined, suggesting a lack of in-control robustness under this particular data scenario. In terms of the shift detection, the ARL_1 values indicate that all charts have similar performances especially when the shift sizes are getting larger.

It is noted that the in-control performances of the MEC- \bar{X} chart and MEC- \tilde{X} chart are unaffected when the underlying process data follow skewed normal-tailed distribution, i.e., $g = 0.5$ and $h = 0$. Table 3 shows that all charts produced $ARL_0 = 370$ when $n = 5$ and $n = 9$. The MEC-MOM chart is observed with an improved ARL_0 as n increases. In term of the shift detection capability, all three MEC charts perform similarly to the normality data scenario.

Finally, the performances of all charts are observed under extreme data conditions, which is $g = 0.5, h = 0.5$, i.e., skewed with the heavy tail distribution. Under this data scenario, the ARL_0 of the MEC- \bar{X} chart is highly affected when compared to the robust MEC- \tilde{X} and MEC-MOM charts. The values in bold in Table 3 are much larger than the pre-determined value of 370. When n increases, the robust MEC-MOM chart

remains unaffected, that is, the values of the ARL_0 are not much different than the pre-determined value of 370. The ARL_0 values for the robust MEC- \bar{X} deviate far from the pre-determined 370 when $n = 5$. As such, this standard MEC chart is no longer reliable for monitoring changes in the process despite showing comparable out-of-control performances with the median based MEC charts. Conversely, both median based MEC charts show good in-control robustness and fast detection when $\delta > 0$, judging by the ARL_0 that is close to 370 and relatively small ARL_1 values as the size of shifts increases, respectively. The finding generally indicates that the in-control

performance of standard MEC- \bar{X} chart is highly affected under heavy-tailed distribution but relatively unaffected otherwise. In contrast, both robust MEC- \bar{X} and MEC-MOM charts perform consistently well in terms of the in-control performance regardless of distributions. Furthermore, the robust MEC-MOM chart performs better under heavy tail distribution regarding the in-control performance while still maintaining its shift detection capability across the normal and non-normal data scenarios.

Table 3 ARL values for the MEC charts with $k = 0.5$ at $ARL_0 = 370$ when process parameters are known

(g,h)	n	Methods	0	0.25	0.5	0.75	1	1.5	2	3
(0,0)	5	MEC- \bar{X}	370.153	27.524	14.525	10.601	8.572	6.453	5.256	4.010
		MEC- \bar{X}	369.980	27.629	14.604	10.679	8.631	6.490	5.288	4.019
		MEC-MOM	370.063	27.534	14.523	10.633	8.599	6.477	5.274	4.017
	9	MEC- \bar{X}	370.091	20.349	11.484	8.527	6.925	5.220	4.222	3.067
		MEC- \bar{X}	370.025	20.582	11.557	8.584	6.970	5.250	4.252	3.086
		MEC-MOM	370.031	20.451	11.545	8.587	6.965	5.241	4.242	3.080
(0,0.5)	5	MEC- \bar{X}	916.526	26.590	14.342	10.501	8.516	6.364	5.108	4.007
		MEC- \bar{X}	369.248	27.585	14.601	10.663	8.632	6.483	5.274	4.018
		MEC-MOM	366.699	27.578	14.549	10.601	8.597	6.460	5.255	4.014
	9	MEC- \bar{X}	976.950	19.921	11.351	8.455	6.961	5.084	4.070	3.016
		MEC- \bar{X}	369.284	20.555	11.573	8.583	6.977	5.244	4.236	3.082
		MEC-MOM	370.789	20.515	11.549	8.561	6.965	5.235	4.236	3.074
(0.5,0)	5	MEC- \bar{X}	372.452	27.588	14.532	10.596	8.584	6.451	5.257	3.990
		MEC- \bar{X}	372.962	27.739	14.625	10.673	8.633	6.488	5.300	3.995
		MEC-MOM	364.845	27.581	14.555	10.617	8.594	6.463	5.290	3.996
	9	MEC- \bar{X}	365.538	20.408	11.472	8.513	6.948	5.212	4.223	3.055
		MEC- \bar{X}	372.261	20.545	11.586	8.571	6.970	5.250	4.257	3.072
		MEC-MOM	373.628	20.537	11.569	8.559	6.969	5.249	4.255	3.076
(0.5,0.5)	5	MEC- \bar{X}	1455.208	26.837	14.302	10.531	8.621	6.413	5.001	3.991
		MEC- \bar{X}	385.235	27.799	14.655	10.693	8.607	6.484	5.291	3.989
		MEC-MOM	378.589	27.694	14.584	10.621	8.614	6.460	5.265	3.989
	9	MEC- \bar{X}	2320.710	19.864	11.341	8.506	6.951	4.994	4.000	2.998
		MEC- \bar{X}	370.140	20.592	11.568	8.578	6.976	5.240	4.249	3.064
		MEC-MOM	377.572	20.589	11.558	8.552	6.972	5.242	4.242	3.061

3.2 Case II: MEC Control Charts with Unknown Parameters

When the in-control parameters of the process are unknown, they have to be estimated based on the historical data in Phase I. Similar to the Case I, the performance of the MEC-MOM, MEC- \bar{X} and MEC- \bar{X} charts are assessed and compared using the ARL. The simulation process in Case II follows similar procedures as in Case I in computing the ARL (Phase

II). An extra step was included prior to that to estimate parameters of the process based on a total subgroup of $m = 50$ with $n = 5, 9$ when $g = 0$ and $h = 0$ (Phase I). Specifically, Phase I involved two series of simulation procedures. The first series was for determining the standard deviation of the sampling distribution of the location estimator, $(\sigma_{\bar{\theta}})$, based on 10^6 iterations. The second series involves 10,000 trials of 50 in-control Phase I with sample size n to estimate the process mean $(\hat{\theta})$.

Let the Phase I data be represented by $X_{ij} = \{X_{1j}, \dots, X_{nj}\}$ where $j = 1, 2, \dots, m$. We assume that X_{ij} to be independent and identically distributed (i.i.d) following an unknown distribution W which has mean θ_0 and standard deviation $\sigma_{\hat{\theta}}$, $X_{ij} \sim W(\theta_0, \sigma_{\hat{\theta}})$. The θ_0 was estimated using the mean of $\hat{\theta}$, given by:

$$\theta_0 = \frac{\sum_{j=1}^m \hat{\theta}_j}{m} \tag{12}$$

The charting constants for different sample sizes (n) are listed in Table 4.

Table 4 The charting constants for different sample sizes (n) when process parameters are unknown

n	MEC- \bar{X}	MEC- \bar{X}	MEC-MOM
5	36.61	37.00	36.74
9	37.00	36.78	36.87

3.2.1 Simulation Outcomes

The ARL results are displayed in Table 4. Focusing on the normal distribution, when $g = 0, h = 0$, all control charts yield $ARL_0 = 370$ as they were initially designed in this study. In terms of the shift detection, all charts perform equally. Moreover, with an increase in the sample size, the value of the ARL_1 decreases for all charts, suggesting an improvement in detecting shifts.

Similar to Case I, even with deviation from the normality assumption, for example, when $g = 0, h = 0.5$, the in-control performance of the robust MEC charts remains unaffected. This is supported by the values of the ARL_0 in Table 5 which are very close to 370. On the other hand, the ARL_0 for the MEC- \bar{X} chart is significantly greater than 370 regardless of the sample sizes examined. In terms of the shift detection, the ARL_1 value indicates that all charts have similar performances in out-of-control status.

It is noted that the in-control performances of both median based control charts, i.e., the MEC- \bar{X} and MEC-MOM charts are not affected when the underlying process data follow skewed normal-tailed distribution, i.e., $g = 0.5, h = 0$, just like in Case I. Table 5 shows that both charts produced $ARL_0 = 370$ when $n = 5$ and $n = 9$. In addition, the out-of-control performance of charts under this data condition are comparable to the standard MEC chart.

Finally, the performances of MEC charts are observed under an extreme data condition, which is $g = 0.5, h = 0.5$, i.e., skewed with heavy tail distribution. The finding indicates that the ARL_0 of the MEC- \bar{X} chart is highly affected when compared to the robust MEC charts. The bold values in Table 5 exceed the pre-determined value of 370. In addition, the ARL_1 of MEC- \bar{X} chart is larger for small shifts ($0.25 \leq \delta \leq 0.75$) when compared to the robust MEC charts. This implies delayed detection by the standard MEC chart when the change in the process is very small. When n increases, the robust MEC-MOM chart remains unaffected, where the values ARL_0 are not much different than 370 suggesting good in-control robustness.

The finding indicates that the in-control robustness of the MEC- \bar{X} chart is highly affected under the heavy-tailed distribution despite being able to perform well under skewed data scenario. In contrast, both robust MEC charts perform consistently in terms of the in-control robustness regardless of underlying distributions. Between the two median based robust charts investigated in this study, i.e., the MEC- \bar{X} and the MEC-MOM chart, the latter performs better under heavy tail distribution in terms of the in-control robustness. With good in-control robustness, the performances of these median based MEC charts are highly reliable in detecting shifts in the process across all distributions considered in this study, unlike the MEC- \bar{X} chart.

Table 5 ARL values for the MEC charts with $k = 0.5$ at $ARL_0 = 370$ when process parameters are unknown

(g,h)	n	Methods	0	0.25	0.5	0.75	1	1.5	2	3
(0,0)	5	MEC- \bar{X}	369.610	37.287	17.397	12.578	10.161	7.629	6.257	4.839
		MEC- \bar{X}	369.824	37.498	17.520	12.662	10.224	7.686	6.294	4.878
		MEC-MOM	369.790	37.156	17.463	12.609	10.188	7.647	6.264	4.848
	9	MEC- \bar{X}	369.438	25.974	13.785	10.206	8.309	6.270	5.123	3.996
		MEC- \bar{X}	370.348	25.808	13.754	10.141	8.279	6.240	5.106	3.994
		MEC-MOM	370.890	25.945	13.759	10.158	8.285	6.251	5.108	3.995
(0,0.5)	5	MEC- \bar{X}	948.992	36.342	17.388	12.610	10.126	7.790	6.130	4.962
		MEC- \bar{X}	371.070	37.663	17.499	12.665	10.204	7.680	6.282	4.891
		MEC-MOM	374.396	37.571	17.446	12.622	10.186	7.639	6.262	4.862
	9	MEC- \bar{X}	1052.478	26.159	13.731	10.187	8.274	6.138	5.030	3.998
		MEC- \bar{X}	371.103	25.877	13.791	10.148	8.295	6.239	5.098	3.993
		MEC-MOM	372.934	25.895	13.791	10.169	8.292	6.256	5.104	3.994
(0.5,0)	5	MEC- \bar{X}	368.318	37.674	17.409	12.619	10.147	7.634	6.256	4.836

(g,h)	n	Methods	0	0.25	0.5	0.75	1	1.5	2	3
		MEC- \bar{X}	370.313	38.376	17.504	12.659	10.230	7.684	6.286	4.864
		MEC-MOM	371.415	37.505	17.511	12.619	10.170	7.639	6.265	4.845
	9	MEC- \bar{X}	379.081	25.938	13.789	10.200	8.309	6.263	5.106	3.990
		MEC- \bar{X}	367.213	25.848	13.752	10.131	8.284	6.240	5.099	3.987
		MEC-MOM	371.620	26.074	13.754	10.182	8.279	6.259	5.099	3.989
		MEC-MOM	1667.373	42.473	18.615	13.053	10.302	7.754	6.041	4.969
(0.5,0.5)	5	MEC- \bar{X}	382.854	38.790	17.572	12.671	10.212	7.679	6.283	4.888
		MEC-MOM	362.879	38.503	17.466	12.619	10.177	7.648	6.260	4.867
	9	MEC- \bar{X}	2845.329	27.619	13.923	10.349	8.112	6.024	4.999	3.998
		MEC- \bar{X}	366.454	25.891	13.790	10.143	8.282	6.233	5.084	3.985
		MEC-MOM	375.956	26.237	13.752	10.170	8.287	6.243	5.086	3.985
		MEC-MOM								

4.0 REAL APPLICATION

To demonstrate the application of the MEC chart on real data, all three charts in this study were applied on a projected rainfall (in milliliter, mm) in Kedah, a state in northwest Malaysia. The data were attained from 2019 until 2020 consisting of 104 samples of size 7 as presented in Figure 1.

The first half of the data was used to construct the control limits (Phase I) and the latter half was used to monitor out-of-control samples (Phase II). For $n = 7$, when the values of λ and k are fixed at 0.13 and 0.5, respectively (as in the simulated studies), h becomes 27.86. The outputs of the proposed charts are given in

Figures 2-4 where both statistics, MEC_t^+ and MEC_t^- , are plotted against the control limits, H and H^- , respectively.

Figure 2 represents the output for the MEC- \bar{X} chart. The chart shows 29 out-of-control samples (samples 14 – 41). Meanwhile, Figure 3 indicates 31 out-of-control samples (samples 11 – 41) MEC- \bar{X} was applied on the data. Figure 4 shows that the output for the robust MEC-MOM chart with 48 out-of-control samples (samples 5 – 52). This implies that the robust MEC- \bar{X} and MEC-MOM charts are more sensitive to the small changes in the data as indicated by this rainfall data scenario.

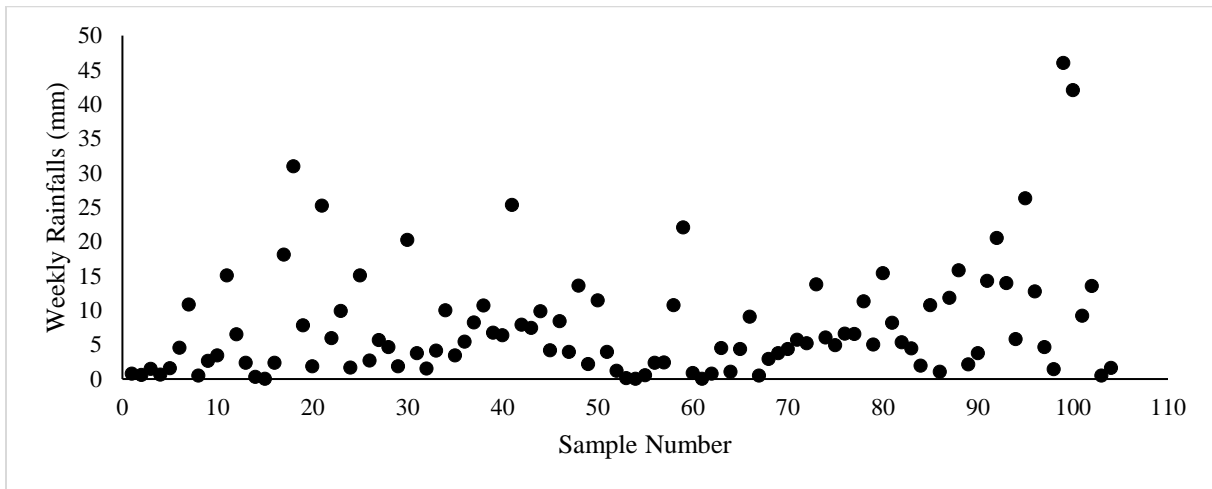


Figure 1 The Scatter Plot of Weekly Rainfalls

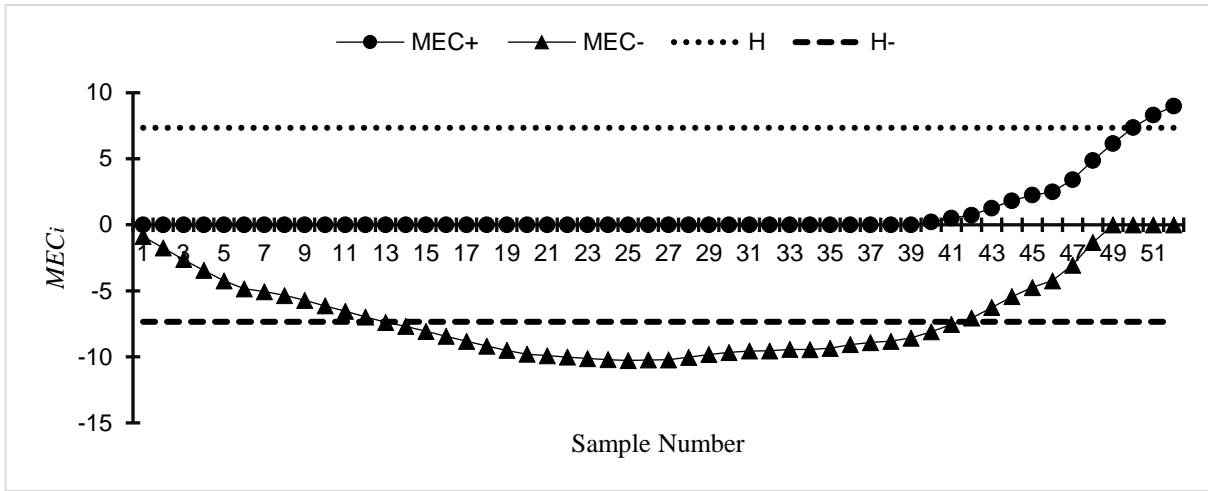


Figure 2 The Standard MEC- \bar{x} Chart

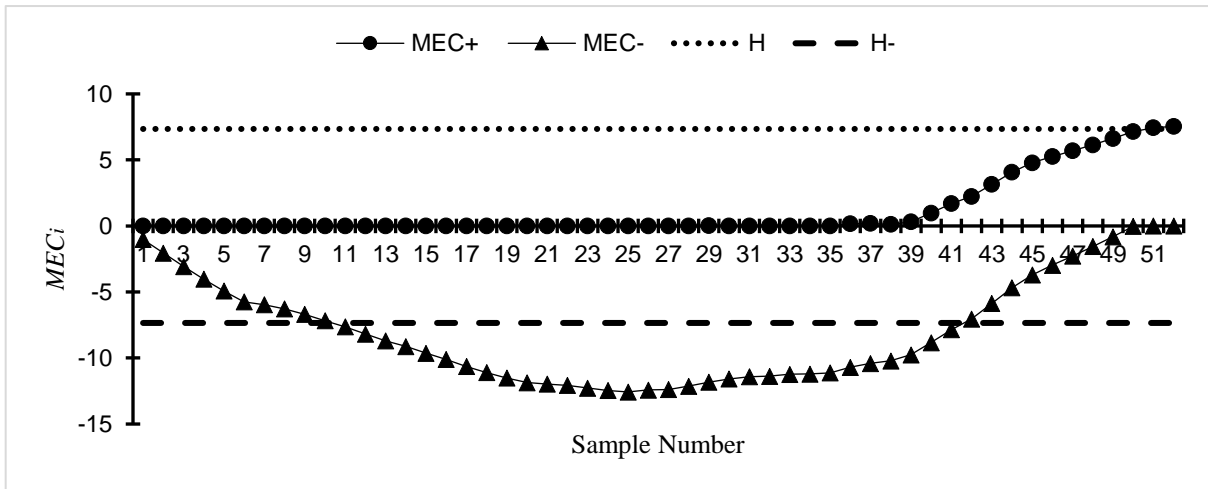


Figure 3 The Robust MEC Chart based on the median

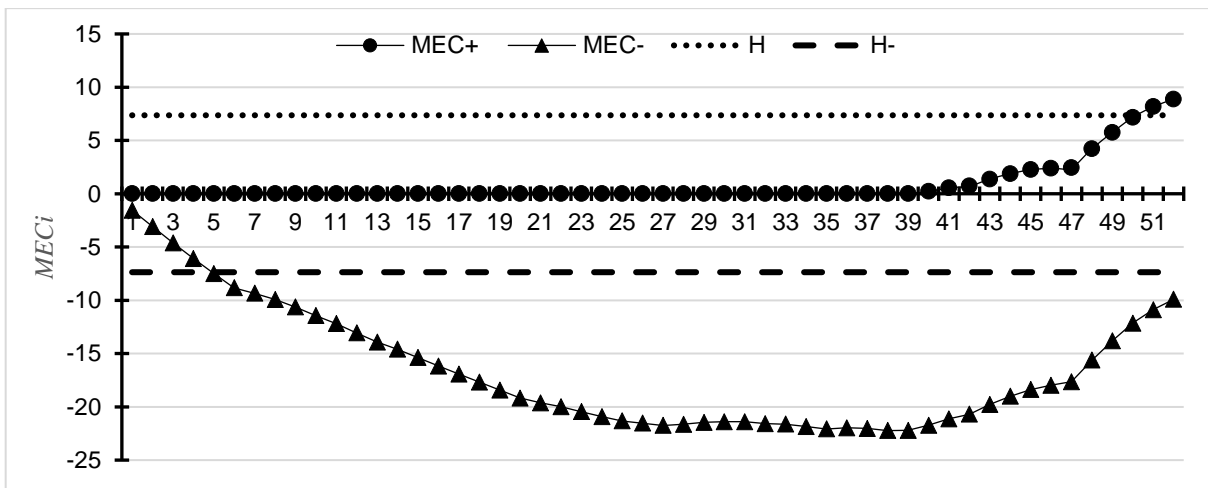


Figure 4 The Robust MEC Chart based on MOM

5.0 CONCLUSION

The MEC control chart is targeted to enhance the performance of the EWMA and CUSUM charts under the normality assumption. This study proposed to improve the performance of the MEC chart under non-normality via the usage of median based estimators. The comparison of the MEC- \bar{X} and MEC-MOM charts with MEC- \bar{X} chart based on the ARL shows that the in-control robustness of the MEC- \bar{X} and MEC-MOM charts are not affected under various g -and- h distributions unlike the MEC- \bar{X} chart. The standard MEC chart, namely, the MEC- \bar{X} chart, is easily perturbed when the distribution is heavy tail in nature. In general, this study observes that MEC- \bar{X} and MEC-MOM charts can withstand various tested conditions and perform well on actual data. The findings indicate that robust MEC-MOM is not easily perturbed regardless of distributional shapes, shifts, and sizes. Thus, they are reliable to be used across various conditions that may be encountered in real life, unlike the MEC- \bar{X} chart.

Conflicts of Interest

The author(s) declare(s) that there is no conflict of interest regarding the publication of this paper.

Acknowledgement

The authors thank Universiti Utara Malaysia for their support in carrying out this research work. This research received no specific grant from any funding agency in the public, commercial, or not-for-profit sectors.

References

- [1] Shewhart, W. A. 1931. *Economic Control of the Quality of Manufactured Products*. Macmillan and Co Ltd, London.
- [2] Hafiz, Zafar, Nazir, Muhammad, Riaz, Muhammad, Riaz, Ronald, J., M., M., Does. 2015. Robust CUSUM Control Charting for Process Dispersion. *Quality and Reliability Engineering International*. 31(3): 369-379. Doi: <https://doi.org/10.1002/qre.1596>.
- [3] Ajadi, Muhammad, Riaz, Khalid, S, Al-Ghamdi. 2016. On Increasing the Sensitivity of Mixed EWMA–CUSUM Control Charts for Location Parameter. *Journal of Applied Statistics*. 43(7): 1262-1278. Doi: <https://doi.org/10.1080/02664763.2015.1094453>.
- [4] Muhammad, Naveed, Muhamma, Azam, Nasrullah, Khan, Muhammad, Aslam. 2018. *Design of a Control Chart Using Extended EWMA Statistic*. 6(4): 108. Doi: <https://doi.org/10.3390/technologies6040108>.
- [5] Hafiz, Zafar, Nazir, Nasir, Abbas, Muhammad, Riaz, Ronald, J., M., M., Does. 2016. A Comparative Study of Memory-type Control Charts under Normal and Contaminated Normal Environments. *Quality and Reliability Engineering International*. 32(4): 1347-1356. Doi: <https://doi.org/10.1002/qre.1835>.
- [6] Wu, T. L. 2018. Distribution-free Runs-based Control Charts. *arXiv preprint arXiv:1801.06532*.
- [7] Zhou, W., Liu, N., & Zheng, Z. 2020. A Synthetic Control Chart for Monitoring the Small Shifts in a Process Mean based on an Attribute Inspection. *Communications in Statistics-Theory and Methods*. 49(9): 2189-2204. Doi: <https://doi.org/10.1080/03610926.2019.1568491>.
- [8] Abdul Rahman, A. 2020. Robust Control Charts Via Winsorized and Trimmed Estimators. Doctoral Dissertation. <https://etd.uum.edu.my/id/eprint/9837>.
- [9] Song Z, Liu Y, Li Z, Zhang J. 2018. A Comparative Study of Memory-type Control Charts based on Robust Scale Estimators. *Quality and Reliability Engineering International*. 34(6): 1079-102. Doi: <https://doi.org/10.1002/qre.2309>.
- [10] Shahid, Hussain, Shahid, Hussain, Xiaoguang, Wang, Shabbir, Ahmad, Muhammad, Riaz. 2020. On a Class of Mixed EWMA-CUSUM Median Control Charts for Process Monitoring. *Quality and Reliability Engineering International*. 36(3): 910-946. Doi: <https://doi.org/10.1002/qre.2608>.
- [11] Atieh, Mahamadkhani, Amirhossein, Amiri. 2020. Developing Mixed EWMA-CUSUM and CUSUM-EWMA Control Charts based on MRSS and DRSS Procedures. *Scientia Iranica*. 0-0. Doi: <https://doi.org/10.24200/sci.2020.55632.4328>.
- [12] Gadde, Srinivasa, Rao, Muhammad, Aslam, Umer, Rasheed, Chi-Hyuck, Jun. 2020. Mixed EWMA–CUSUM Chart for COM-Poisson Distribution. *Journal of Statistics and Management Systems*. 23(3): 511-527. Doi: <https://doi.org/10.1080/09720510.2019.1639947>.
- [13] Nasir, Abbas, Muhammad, Riaz, Muhammad, Riaz, Ronald, J., M., M., Does. 2013. Mixed Exponentially Weighted Moving Average-Cumulative Sum Charts for Process Monitoring. *Quality and Reliability Engineering International*. 29(3): 345-356. Doi: <https://doi.org/10.1002/qre.1385>.
- [14] Abdul Rahman, A., Syed Yahaya, S. S., Atta, A. M. A. 2019. Robustification of CUSUM Control Structure for Monitoring Location Shift of Skewed Distributions based on Modified One-step M-estimator. *Communications in Statistics-Simulation and Computation*. 14: 1-8. Doi: <https://doi.org/10.1080/03610918.2018.1532001>.
- [15] Abdul Rahman, A., Syed Yahaya, S. S., Atta, A. M. A. 2018. A Robust CUSUM Control Cumulative Sum Control Chart for Monitoring the Process Mean based on a High Breakdown Point Scale Estimator. *Journal of Engineering and Applied Sciences*. 13(10): 3423-3429. Doi: <https://doi.org/103923/jeasci.2018.3423.3429>.
- [16] Abdul Rahman, A., Syed Yahaya, S. S., Atta, A. M. A. 2018. Monitoring Mean Shift of Skewed Distributions Using Modified One-Step M-estimator with EWMA Control Structure. *Journal of Theoretical and Applied Information Technology*. 96(13): 4004-4019.
- [17] Noor, N. F. M., Abdul-Rahman, A. Y. U., & Ali, A. M. 2023. The Effectiveness of Robust Mixed EWMA-CUSUM Control Chart on g -and- h Distribution. *Journal of Theoretical and Applied Information Technology*. 101(13): 5122-5129.
- [18] Castagliola, P. 2001. An-EWMA Control Chart for Monitoring the Process Sample Median. *International Journal of Reliability, Quality and Safety Engineering*. 8(02): 123-135. Doi: <https://doi.org/10.1142/S0218539301000414>.
- [19] Abdul Rahman, A., Syed Yahaya, S. S., & Atta, A. M. A. 2018. The Effect of Median based Estimators on CUSUM Chart. *Journal of Telecommunication, Electronic and Computer Engineering*. 10(1-10): 49-52. <https://repo.uum.edu.my/id/eprint/24403>.
- [20] Abdul Rahman, A., Syed Yahaya, S. S., Atta, A. M. A., Ahad, N. A., & Hamid, H. 2020. The Impact of Data Anomaly on EWMA Phase II Performance. *Journal of Engineering and Applied Sciences*. 15(15): 3010-3015. <https://repo.uum.edu.my/id/eprint/27552>.
- [21] Abdul-Rahman, A., Syed-Yahaya, S. S., & Atta, A. M. A. 2021. Robust Synthetic Control Charting. *International Journal of Technology*. 12(2). Doi: <https://doi.org/10.14716/ijtech.v12i2.4216>.
- [22] E., S., Page. 1954. Continuous Inspection Schemes. *Biometrika*. 41: 100-115. Doi: <https://doi.org/10.1093/biomet/41.1-2.100>.
- [23] Montgomery, D. C. 2009. *Introduction to Statistical Quality Control*. 6th ed. John Wiley & Sons Inc. 45-60.
- [24] S., W., Roberts. 2000. Control Chart Tests based on Geometric Moving Averages. *Technometrics*. 42(1): 97-101. Doi: <https://doi.org/10.2307/1271439>.